Degenerate time-dependent network dynamics anticipate seizures in human epileptic brain

Adrià Tauste Campo[1,2], Alessandro Principe[2], Miguel Ley[2], Rodrigo Rocamora[2,3*] and Gustavo Deco[1,4*]

1 Computational Neuroscience Group, Universitat Pompeu Fabra (UPF), Barcelona, Spain
2 Epilepsy Monitoring Unit, Department of Neurology, Hospital del Mar Medical Research (IMIM), Barcelona, Spain
3 Faculty of Health and Life Sciences, Universitat Pompeu Fabra (UPF), Barcelona, Spain
4 Institució Catalana de Recerca i Estudis Avançats (ICREA), Barcelona, Spain

[*] These authors contributed equally to this work.

Correspondence to: Adrià Tauste Campo,
Institut Hospital del Mar d'Investigacions Mèdiques
Barcelona Biomedical Research Park
C/ Dr. Aiguader, 88
08003 Barcelona
Spain

Abstract

Epileptic seizures are known to follow specific changes in brain dynamics. While some algorithms can nowadays robustly detect these changes, a clear understanding of the mechanism by which these alterations occur and generate seizures is still lacking. Here, we provide evidence that such changes are initiated by an alteration of physiological network state dynamics. Specifically, our analysis of long intracranial EEG recordings from a group of 10 patients identifies a critical phase of a few hours in which time-dependent network states become less variable ("degenerate") and is followed by a global functional connectivity reduction before seizure onset. This critical phase is characterized by an increased presence of high-connected network states and is shown to particularly constraint the activity of the epileptogenic zone in patients with validated good post-operative outcome. Our approach characterizes pre-seizure networks dynamics as a cascade of two sequential events providing new insights into seizure prediction and control.

Epilepsy is among the most common neurological disorders with an estimated prevalence of about 1% of the world's population and almost 2% in low-income families in developed countries (CDC, 2010). Epilepsy is characterized by the seemingly random occurrence of seizures, which can greatly affect the quality of life of patients. Approximately one third of all epileptic patients are resistant to pharmacotherapy (Patrick *et al.*, 2011) and could benefit

from a variety of surgical options. Among them, closed-loop neuromodulation based on an accurate prediction of seizure occurrences is a promising tool.

Over the last decades, several studies have showed that seizures are preceded by detectable changes in brain dynamics that can be measured via intracranial recordings. Although not being fully understood, these changes have been associated to the existence of a transition from interictal activity to *pre-ictal state* (Lopes da Silva 2003, Stacey *et al.*, 2011). These findings have motivated intense research on the development of seizure prediction algorithms for therapeutic use in patients with refractory epilepsy (Park *et al.*, 2011, Valderrama *et al.*, 2012, Cook *et al.*, 2013, Gadhoumi *et al.*, 2015). Although significant progress has been made to attain above-chance level performance results (Brinkmann *et al.*, 2016), there is yet a long road to turn seizure prediction into therapeutic devices. A major caveat of current seizure prediction is the lack of understanding about the neurophysiological processes associated to the emergence and maintenance of the pre-ictal state. Indeed, most studies have resorted to fully data-driven methods to discriminate the pre-ictal state with multiple signal features, which are typically patient-specific and difficult to interpret (Gadhoumi *et al.*, 2015).

Nowadays epilepsy research is gradually adopting a network approach to study seizure dynamics at a global level and assess the contribution of the epileptogenic zone (Van Diessen *et al.* 2013, Van Mierlo *et al.*, 2014, Goodfellow *et al.*, 2016, Khambati *et al.,* 2016). In this growing field, the majority of published studies have identified specific graph-theoretical properties of functional networks during ictal and interictal periods (Kramer *et al.*, 2008, Bartolomei *et al.*, 2011, Haneef *et al.*, 2014, Stam 2014). More recently, a few groups have highlighted the critical dependence of these findings into the dynamics of brain network states (Takahashi *et al.*, 2012, Rummel *et al*. 2013, Burns *et al.*, 2014, Khambati *et al.,* 2015). However, some questions remain open. How are physiological network states dynamically altered before epileptic seizures? Can network dynamics provide a common principle of the pre-ictal state?

In the current study, we tackled these questions by analyzing time-dependent alterations in the dynamic repertoire of the functional connectivity (Hutchinson *et al.*, 2013) during long pre-seizure periods. More specifically, we hypothesized that the variability of network states

measured via graph-theoretical analysis was altered before epileptic seizures. Under this hypothesis, we developed a method to study specific variability changes prior to seizures preceded by long interictal periods in 10 epileptic patients monitored with video-SEEG (stereoencephalography) during pre-surgical diagnosis. We made use of a graph-theoretical property, the eigenvector centrality, to characterize network states (Burns *et al.*, 2014) as instances of a time-varying multivariate continuous variable, and resorted to the Gaussian entropy (Cover and Thomas, 2012) to describe their variability. A controlled analysis using the pre-seizure period and a day-matched period from the previous day revealed a consistent and sustained decrease of the variability of network states before the seizure occurred. Remarkably, in all patients this loss of variability was associated to a higher presence of high-connectivity states during the pre-seizure period. We also investigated the contribution of the epileptogenic sites to the observed effect in three patients with a very good post-operative outcome and a sufficiently long follow-up period. In particular, the application of our analysis to the mapped epileptogenic of seizure-free patients showed a significant and specific decrease in the temporal variability of their network activity. Overall, our approach provides two contributions in the analysis of epileptic network dynamics. First, it characterizes the pre-ictal state as an alteration of physiological network dynamics that provokes functional changes before seizures. Second, it develops methodological aspects that may be considered to improve seizure prediction algorithms. More broadly, the results presented here open new lines to investigate critical alterations in pathological networks by studying the time-varying nature of brain networks.

Results

We studied network dynamics prior to epileptic seizures in 10 drug-resistant patients using continuous multichannel intracranial recordings via stereoelectroencephalography (SEEG) during pre-surgical monitoring evaluation (See details in Table 1). To capture long-term changes in network dynamics, we considered patients whose first spontaneous clinical seizure occurred after at least 30 hours (average value: 71.4±19.1 hours; mean±std) of intracranial implantation. This ictal activity exhibited variable onset times over patients that were more concentrated during the 0:00-8:00 period (Fig. 1A). For every patient, we analyzed a long continuous period (average value: 10.4±1.9 hours; mean±std) of intracranial activity before the seizure occurred (pre-seizure period, Fig. 1B). We controlled for the specificity of our

findings by independently analyzing a daytime matched period of interictal activity from the precedent day (control period, Fig. 1B). In this study we could include 3 patients with very good post-surgical outcome after a minimal follow-up of 1.5 years (Patients 1-3) and two patients that presented potential perturbation factors affecting the pre-seizure period (Patients 9 and 10). More precisely, Patient 9 had been electrically stimulated 16.5 hours before the first recorded seizure and Patient 10 presented a subclinical seizure 6.1 hours before the first clinical seizure onset.

Network dynamics analysis

We tracked network dynamics for each patient separately over each SEEG recording session. To do so, we computed the functional connectivity across all recording sites (also referred to as sites, average value: 98.3±25.1 sites; mean±std) over consecutive and non-overlapping time windows of 0.6s (Fig. 1D). Networks in each window were characterized as a weighted directed graph, where electrode contacts represented the nodes and absolute-valued pairwise correlations represented their weighted edges (Fig. 1D). We then evaluated a centrality measure for each connectivity matrix to track network dynamics in a reduced and interpretable dimensionality space. Indeed, we computed the eigenvector centrality to reduce each $N \times N$ connectivity matrix to a N-dimensional vector, where N was the total number of recording sites, thus obtaining a centrality sequence for each recording site (Fig. 1D).

Our initial hypothesis was that the pre-ictal state was associated with an alteration of physiological network states. We therefore tested this hypothesis by quantifying changes in the distribution of the eigenvector centrality sequences representing these network states. In particular, we assumed that the centrality time series could be approximated by a multivariate Gaussian distribution for a sufficiently large number of samples (n>100). In principle, the second-order variability of a multivariate variable may exhibit two components: the temporal component, i.e., how the centrality of a recording site varies as a function of time, and the spatial component, i.e., how the centrality consistently varies across recording sites at given time instance. A measure that simultaneously quantifies both components is the multivariate Gaussian entropy, which monotonically depends on the product of the covariance matrix's eigenvalues (Fig. 1C). This measure corresponds to the differential entropy of multivariate normally distributed variables (Cover and Thomas, 2012), and it can be proved useful to approximate the variability of more general variables in the large-sample regime.

Network state variability identifies a physiologically altered period hours before seizure onset

Over each period of interest (pre-seizure, control), we computed the multivariate Gaussian entropy in consecutive and non-overlapping time windows of 200 centrality samples (120s) and normalized the measure to lie within the interval [0,1] per patient. We shall refer to this applied measure as centrality entropy in the remaining of the article. The straightforward application of the centrality entropy to both periods showed that centrality sequences were generally less entropic during the pre-seizure period (See Fig. S1) showing a gradual increase and decrease of this cross-period difference as seizure onset approached. In order to localize this effect in a specific and significant time segment, we grouped consecutive entropy values into intervals and made use a non-parametric test to identify the cluster of consecutive centrality entropy intervals that was significantly yielding the largest entropy decay per patient (*Materials and methods*). The results of this test are illustrated for all patients in Fig. 2A where average centrality entropy curves are plotted for the control (in blue) and pre-seizure period (in red) together with the identified significant time segment (in cyan) during the 9.5 hours preceding the seizure. In each patient, this segment highlighted intervals where the same centrality entropy reduction could not be achieved by shuffling interval-dependent entropy values across the pre-seizure and control periods ($P<0.01$, Fig S2A). Intriguingly, the identified segment was rather patient-specific exhibiting offset times that were not generally attached to the seizure onset. However, when grouping samples across patients 1-9, significant intervals turned out to be regularly distributed around the proximity of the seizure onset with the interval [-2.5, -2] being the most frequent (Fig. 2B). In particular, this distribution was statistically different ($P<0.05$, Kolmogorov Smirnov test) from a surrogate distribution obtained by randomly placing the same segments per patient in every possible location of the pre-seizure period (Fig. 2C). In addition, relevant features of the identified segment such as the onset and offset times, and the test's statistic value were not significantly correlated with the seizure onset time (Fig. S2B, C and D), which excluded a straightforward association of the observed effect with daily rhythms. Finally, the results obtained in both patients with potential perturbation factors were rather different. Interestingly, Fig. S2A quantified the cross-period difference measured in Patient 9 to be the least significant across all patients, suggesting that a previous received electrical stimulation might have had an effect on his pre-seizure dynamics. In contrast, the occurrence of a subclinical seizure in Patient 10 did not yield a qualitatively different result. These initial findings suggested that

significant sustained reductions of network state variability over a precedent-day baseline could serve as a biomarker to anticipate seizures. Further, this reduction in variability was statistically mapped to a patient-specific time period per patient that will be referred to in the following as the critical phase.

As observed earlier, the critical phase was not in general attached to the seizure onset of every patient. Hence, how could the critical phase be related to the reported evidences of the pre-ictal state? To address this question, we split both recording sessions of Patients 1-9 into the critical phase, and sub-periods immediately before (pre-critical phase) and after (post/ending critical phase) the critical phase (Fig. 2C). For those patients with critical phases attached to the seizure onset (Patients 1, 6 and 8) we considered the post-critical phase to comprise the last window time samples of the critical phase. In each sub-period we evaluated the mean functional connectivity along both recording sessions. The results shown for patients with recorded pre-critical and critical phases reveal that during the critical phase of the pre-seizure period the mean connectivity exhibited an increase that was not significant over these patients (Fig. 2C, $P>0.05$, paired Wilcoxon test, $n=8$). In contrast, when comparing the critical and the post/ending-critical phases the mean connectivity decreased significantly over all patients (Fig. 2C, $P<0.01$, paired Wilcoxon test, $n=10$), which conciliates with previous characterizations of the pre-ictal state (Mormann *et al.* 2003, Le Van Quyen *et al.*, Stacey *et al*, 2011). Interestingly these variations were not present during the control period, suggesting that the global connectivity decrease was specific of the pre-seizure period and could be driven by the critical phase.

Reduced network state variability spans across spatial and temporal scales

As introduced earlier, the centrality entropy quantified the (spatio-temporal) variability of simultaneous centrality sequences in a single scalar value. Then, how was the variability reduction individually expressed along recording sites and along time samples? To answer this question, we repeated the previous non-parametric statistical analysis (Fig. 2A) over both recording periods using the spatial and temporal versions of centrality entropy independently (*Materials and methods*). Although the results were generally reproduced along each dimensions the variability reduction was differently distributed across space and time over patients. A patient's classification based on the pairing of the spatial and temporal statistical effects (green dots, Fig. 3B) highlighted patients in which the variability reduction was

mainly temporal (Fig. 3C, Patient 2), patients where the sites' centrality became more homogeneous (Fig. 3C, Patients 3 and 8), and a patient where the effect equally spanned over both dimensions (Fig. 3C, Patient 5). In sum, the decrease of network state variability observed during the pre-seizure period was associated to the occurrence of more similar centrality values over time (less temporal variability), which in general exhibited more homogeneous centrality values across recording sites (less spatial variability).

High-connectivity states significantly increase during the critical phase.

The previous results described that network states (as modeled by the eigenvector centrality measure) became more temporally redundant and more spatially homogeneous (Fig. 3) during the critical phase. In turn, the reduced spatio-temporal variability was associated to a non-significant increase of the mean connectivity across patients (Fig 2C). Yet, how was the actual interplay between network dynamics and connectivity alterations during the pre-seizure period? An initial analysis based on the time-dependent mean connectivity (averaged over all recording sites' pairs) did not reveal consistent cross-period differences over patients (Fig. S5). Then, we related the observed reduced network variability to alterations in the associated connectivity of certain states. In particular, were there specific time-varying states producing this effect? We initially tackled the question from a qualitative perspective and inspected the eigenvector centrality sequences during the control and pre-seizure periods. A visual inspection on these vector sequences for every patient suggested that the amount of highly homogeneous vectors (represented as yellow strips in the plot) was larger during the pre-seizure period and that these homogeneous vectors were associated with high-connectivity matrices in the majority of patients (Fig. 4A).

Vector sequences like the one presented in Fig. 4A showed that network states transited instances that were similarly repeated over time. Then, we used a clustering algorithm to extract the eight most representative vectors over both periods of interest and classified each centrality vector at any given time accordingly (*Materials and methods*). Consequently, the sequence of centrality vectors turned into a sequence of discrete states whose frequency over any time interval (probability) could be computed and compared across control and pre-seizure periods (Fig. 4B). Based on these states probabilities, we correlated the main observed effect with consistent differences in the probability of each discretized state across both periods. More specifically, for each state we correlated its probability difference with

the reduction in centrality entropy partialling out the effect of the remaining states. The application of this procedure at a single-patient level provided a correlation coefficient per state (Fig. 4B). To investigate the influence of every state's connectivity into this association over patients, states were sorted in decreasing connectivity order and patient's correlations coefficients were distributed in boxplots for each state (Fig. 4C). Interestingly, Fig. 4C shows that the probability of the highest connectivity states was negatively correlated with the centrality entropy decrease (median coefficient=-0.22, median p-value=2.1e-4) indicating that the higher occurrence of these states during the pre-seizure period was related to the network variability reduction in the majority of patients. In particular, the influence of the highest connectivity state occurrence into the variability decrease was consistently significant in 7 out of 9 patients ($P<0.01$, partial correlation). In the remaining two patients, the largest influence was found in the second-highest (Patient 2) and the third-highest connectivity states (Patient 5) respectively. Then, for each patient we focused on the states whose probability increase during the pre-seizure period significantly correlated with the entropy decrease, and denoted as high-connectivity states (HCS) the ones among those that were associated with the highest connectivity matrix. In particular, when restricted to the critical phase (Fig. 2A), the probability of high-connectivity states was significantly increased during the pre-seizure period ($P<0.01$, paired t-test, Fig. 4D).

Epileptogenic zone is functionally altered during the critical phase

Importantly, the alteration of network dynamics observed during the pre-seizure period could be associated to a time-dependent common factor (greater occurrence of HCS) in all patients. Yet, how this consistent alteration could evolve into generating seizures? In particular, how was this effect manifested in those regions that were involved in seizure generation? To further relate our findings to the ictogenesis process we particularized our analysis to the clinically mapped epileptogenic zone of three patients with good post-operative outcome and a follow-up period of more than one and a half years (*Materials and Methods*, Table 1). Two out of these patients are seizure free (Patients 1 and 2) while the remaining patient (Patient 3) exhibits reduced ictal symptomatology (seizure auras). In these patients, we specifically investigated the relationship between the overall network variability decrease during the pre-seizure period and the dynamics of the epileptogenic zone in control and pre-seizure segments. To carry out this region-specific analysis, we first evaluated the temporal mean and standard deviation of the recording sites' centrality in the epileptogenic zone (EZ) and in the

non-epileptogenic zone (NEZ) over the control and pre-seizure periods. Fig. 5A plots the time-average centrality in the 3 patients as a function of the remaining time to seizure onset. Interestingly, this figure qualitatively illustrates that the time-average centrality of the EZ was higher than the NEZ over each period of interest and that cross-period trajectory deviations occurred in both regions during the assessed critical phase (Fig. S1, in cyan). These preliminary observations suggested that both regions were involved in the pre-ictal dynamics despite having different functional roles. However, were both regions equally involved? Fig. 5B characterizes both regions dynamics by comparing the temporal standard deviation of their recording site's centrality across EZ (inner left) and NEZ (inner right) regions, recording periods and inside (outer left) and outside (outer right) the critical phase. To assess statistical differences between regions that were robust to the different small sample we resorted to the effect size measured by Cohen's D and highlighted comparisons exceeding the value of 0.3 (medium effect, Cohen, 1992). Using this statistical analysis, Fig 5B shows in both seizure-free patients (Patients 1 and 2) that the largest decrease in the centrality variability (D>0.3) was localized in the EZ during the critical phase. In contrast, the effect's magnitude in patient 3 (patient still exhibiting ictal symptomatology) was similar in both regions during the same critical phase. Outside the critical phase, cross-period comparisons included differences of opposite sign but none of them attained the same effect sizes. These results supported the idea that alterations of the EZ dynamics were actively contributing to the variability reduction observed at a whole network level.

We finally investigated the influence of HCS on epileptogenic and non-epileptogenic sites to further describe the functional alterations occurring during the critical phase. More specifically, we compared the average connectivity per site (known as strength) in the EZ and NEZ during the presence of the HCS and the remaining states (non-HCS) in each patient (Fig. 5C). The strength of the EZ was higher than that of the NEZ in all patients during non-HCS condition (D=0.92, 0.4, 0.51, Cohen's D). In contrast, during the HCS, recording sites were more homogeneously connected and the strength difference between EZ and non-EZ notably shrank showing a strongest decay in patients 1 and 3 (D=0.38, 0.36, 0.28, Cohen's D). Therefore, during the critical phase, the higher occurrence of HCS was altering the intrinsic connectivity gradient between the EZ and non-EZ .

Discussion

This study examined the existence of a common alteration principle in brain network dynamics during long-lasting periods of activity preceding the first clinical seizure in 10 patients with focal refractory epilepsy. Using a comparative analysis between genuine pre-seizure periods and a time-matched period from the precedent day per patient, we were able to consistently show a sustained decrease in the variability of network states that was followed in most of the patients by a functional connectivity drop before the seizure onset. Further analysis revealed factors altering this variability in the temporal (time samples) and spatial (recording sites) domains. First, this decrease in network variability was associated with an increased presence of high-connectivity states during pre-seizure periods. Second, the reduction in temporal variability was mainly localized in the mapped epileptogenic zone of the two patients with best post-operative outcome.

The work presented here makes use of a novel approach to quantify the network dynamics alterations that occur during the pre-ictal period. Over the last decade, fMRI studies have showed growing evidence that dynamic connectivity patterns ("brain dynamic repertoire") may be an intrinsic property of brain function and disease (Hutchinson *et al.*, 2013). Particular examples of disrupted dynamics have been found in Alzheimer's disease (Jones *et al.*, 2012) and neuropsychiatric disorders (Damaraju *et al.*, 2014) whose translation to new clinical biomarkers is currently matter of discussion (Deco and Krigelback 2014, and references therein). In modern epilepsy research, the dynamic principle of brain function has been postulated to be commonplace to understand the ictogenesis process (Richardson 2012) but most network studies have studied alterations in static functional networks with a few exceptions (Dimitriadis *et al*., 2012, Morgan *et al.,* 2015).

When studying the variability of brain dynamics along long recording periods, one is confronted with the confounding effect of circadian rhythms (Kuhnert *et al.*, 2010, Rocamora *et al.*, 2013, Geier *et al.*, 2015), which span across sleep and wake phases. These rhythms may become critical when one characterizes specific brain configurations associated with the pre-ictal state, which has been shown to approximately last 4 hours (Mormann *et al.*, 2007). Previous studies on the pre-ictal state have analyzed pre-ictal changes with reference to previous interictal periods, not necessarily time-matched. Inspired by a previous work (Andrzejak *et al.*, 2003), the strategy used here tackled this issue by defining a time-matched

reference period from the precedent day, thus allowing for a more specific identification of pre-ictal changes in brain network dynamics. Nonetheless, the existence of time-locked brain dynamics at the scale of tenths of minutes is an assumption that may not suffice to control for all physiological phase transitions. Hence, whether degenerate network dynamics were produced by time shifts in sleep/awake phase transitions across both days or a change within a single sleep/wake phase was not fully addressed in this study. Yet, our preliminary results on the relationship between patient's putative critical phases and seizure onset times do not seem to support the phase time-shift hypothesis. In any event, a larger cohort of patients with variable seizure times and a good readout of their sleep phases will be necessary to address this question in the future. Another key aspect of the study is the use of the first monitored clinical seizure occurring during the first 2-3 implantation days. This choice was pivotal to analyze comparable long-term network dynamic changes across patients with limited influence of confounding factors such as the reduction of antiepileptic drugs, the effect of previous ictal processes and the response to clinical stimulation.

A central question in seizure prediction research has been the role of synchronization (Jiruska *et al.*, 2013) during the pre-ictal period. Some studies have reported drops in synchronization a few hours before seizure onset (Mormann *et al.*, 2003) while others have pinpointed the coexistence of distinct synchronization states depending on the recorded structures (Le Van Quyen *et al.*, 2005, Van Mierlo *et al.*, 2014). Even though a clear mechanism of such alterations is still missing, the most successful algorithms applied to large data sets make use of correlation matrices as key data features (Binkmann *et al.*, 2016). The findings presented in this study support the view that pre-ictal correlation patterns are state dependent and hence, their alterations should be interpreted according to underlying state dynamics (Le Van Qyuen *et al.*, 2005, Takahashi *et al.*, 2012). More specifically, they suggest that a time-dependent excess of high correlation states may be at the origin of the pre-ictal period.

Over recent years there is accumulated evidence that seizure generation and spread involves complex interactions between seizure-generating and surrounding areas (Rummel *et al.* 2013, Khambati *et al.,* 2015, Khambati *et al.,* 2016). Evaluating network dynamics in patients with good post-surgical outcome, we were able to relate our findings to both the clinically mapped epileptogenic zone and the remaining areas. In these patients the average contacts' centrality was higher in the epileptogenic zone than in the non-epileptogenic zone for the entire

analyzed periods in line with previous studies (Wilke *et al.*, 2011, Van Mierlo *et al.*, 2013). Not surprisingly, changes in this average centrality level across periods occurred during the assessed critical phase where both regions deviated from their control-period trajectories. Crucially, this change in the time-average centrality was accompanied by a significant and specific decrease in the centrality (temporal) variability of the epileptogenic zone, which was prominently present in the two seizure-free patients. Instead, the patient that was not completely seizure-free showed an unspecific decrease, which corroborates that his epileptogenic zone might have not been fully mapped. The analysis on the influence of high-connectivity states into the epileptogenic zone showed that these states exhibited homogenous connectivity strength across regions and provided initial evidence that a higher occurrence of these states may destabilize the intrinsic functional balance between epileptogenic and non-epileptogenic regions observed in the three studied patients. We hypothesize that this network state degeneracy particularly affects the functional activity of the epileptogenic network prior to seizures. Yet, a larger study including more seizure-free patients will be necessary to fully elucidate the mutual influence between physiological network dynamics and the epileptogenic zone.

The results shown in this study prompt to further investigate the exact physiological origin of such alterations considering putative factors like sleep deprivation or antiepileptic drugs reduction. A number of considerations are yet to be mentioned. First, the use of intracranial recordings is a limiting factor in the spatial analysis of brain states, thus making them a priori subject-dependent. Nonetheless, it is recognized that the SEEG methodology offers an optimal temporal and spatial resolution of neurophysiological recordings for neural signal analysis in comparison with other techniques in patients with epilepsy. Second, the functional connectivity analysis relied on a linear coupling measure and was frequency independent. Although this approach was sufficient to characterize network states, we expect that the overall analysis may benefit from considering non-linear coupling measures applied at certain frequency bands. In conclusion, this work provides electrophysiological evidence for characterizing the pre-seizure period as a long-lasting process in which time-dependent network dynamics are degraded provoking a functional reorganization of epileptic networks before seizure onset. Further investigations under this conception will help unravel seizure generation mechanisms from a network perspective, provide practical insights into how to

predict and control ictal activity, and may constitute a general approach to analyze dynamic alterations of other neuropathologies.

Materials and Methods

Patients and recordings

A total number of 203 hours of SEEG recordings from ten patients with pharmacoresistant focal-onset seizures were analyzed. A summary of the patients' characteristics is given in Table 1. We included patients who presented the first seizure in a time frame that allowed us to perform a controlled analysis of EEG recordings during the pre-seizure period. Specifically, each patient in the study was selected if her first video-SEEG monitored clinical seizure had occurred after at least 30 hours (average value: 71.4±19.1 hours; mean±std) with no presence of spontaneous clinical seizures. Among the selected patients we included two patients presenting potential perturbation factors affecting the pre-seizure period (Patients 9 and 10). Patient 9 had been electrically stimulated 16.5 hours before the first recorded seizure and Patient 10 presented a subclinical seizure 6.1 hours before the first clinical seizure onset.

For each patient, the selection of recording sessions was as follows. We considered up to 12 hours before the first monitored clinical seizure occurred. As a baseline reference, we selected the same time period from the previous day (control period). After detecting recording cuts in a few patients, we restricted the analysis to 11 hours per session in patients 1-9 and to 2.4 hours per recording session in patient 10 to ensure a time-matched cross-period comparison. Among the selected patients, two patients achieved seizure freedom after surgical resection and radiofrequency thermocoagulation (RFTC, Cossu *et al.* 2015) with a follow-up of 3 years and 1.5 years respectively (Patients 1 and 2, Engel 1A). An additional patient only exhibited seizure auras after surgical resection and a follow-up of 3 years (Patient 3, Engel 1B). We considered these three patients (Patients 1-3) to have a validated very good post-operative outcome (Engel 1 or 2). Hence, for the purpose of the analysis presented here we considered the diagnosed seizure onset zone and the operated zone of these three patients to be included in their epileptogenic zone. The remaining patients had a non-sufficiently follow-up period (<6 months, Patients 4, 5, 6 and 8), had not been operated (Patient 7) or exhibited a bad post-operative outcome (Patients 9 and 10).

All recordings were performed using a standard clinical EEG system (XLTEK, subsidiary of

Natus Medical) with a 500 Hz sampling rate. A uni- or bilateral implantation was performed accordingly, using 5 to 15 intracerebral electrodes (Dixi Médical, Besançon, France; diameter: 0.8 mm; 5 to 15 contacts, 2 mm long, 1.5 mm apart) that were stereotactically inserted using robotic guidance (ROSA, Medtech Surgical, Inc).

Data pre-processing

EEG signals were processed in the referential recording configuration (i.e., each signal was referred to a common reference). The sets of electrodes included in this analysis are reported in Table 1 and displayed in Fig. 1 (top row). All recordings were filtered to remove the effect of the alternate current (Notch at 50 Hz and harmonics using a FIR filter). Then signals were further band-pass filtered between 1Hz and 150 Hz to remove slow drifts and aliasing effects respectively. Artifacts were removed in each period by detecting time window samples 600ms) where mean correlation values and recording site average signal amplitudes were 3 standard deviations larger than their median values across each period.

To perform functional connectivity analysis each EEG signal was divided into consecutive and non-overlapping 0.6s-long windows (300 samples with 500Hz sampling rate) to balance the requirements of approximate stationarity of the time series (requiring short epochs) and of sufficient data to allow accurate correlation estimates (requiring long epochs).

Functional connectivity analysis

There are different methods to assess functional connectivity from time series data based on coupling measures (Pereda *et al.*, 2005, Wendling *et al.*, 2009). Previous research on the comparison of linear and non-linear coupling measures has resulted in having distinct "ideal" measures for distinct studied situations (Stefan *et al.*, 2013). Here we chose to employ a zero-lagged linear correlation measure for its good tradeoff between simplicity and robustness (Wendling *et al.*, 2009) and because it allowed for a simple definition of network states.

Let $x(n)$ and $y(n)$ be two N-length time series representing two recorded signals during 0.6-s long epoch and let $\underline{x}$ and $\underline{y}$ be their respective time means. Their sample (Pearson) is estimated as

$$r(x,y) \triangleq \frac{\sum_{i=1}^{N}(x(i)-\bar{x})(y(i)-\bar{y})}{\sqrt{\sum_{i=1}^{N}(x(i)-\bar{x})^2}\sqrt{\sum_{i=1}^{N}(y(i)-\bar{y})^2}} \tag{1}$$

For each patient and each consecutive 0.6s-long window we computed the absolute value of the coupling measure across all pairs of electrode contacts. For most of the patients, the overall pairwise computations resulted in approximately 123000 sequential connectivity matrices combining both recording sessions (control and pre-seizure periods). In the current study, we did not test the statistical significance of each pairwise coupling since our purpose was to track the overall network dynamics regardless of pairwise thresholding methods.

Network analysis

For each patient, we characterized each connectivity matrix as a network. This network was modelled as a weighted undirected graph, where electrode contacts represented the nodes and pairwise correlation values across represented their weighted edges (Ponten *et al.*, 2007). Then, we computed the network measure of eigenvector centrality for each connectivity matrix (Newman, 2010). For a given graph, $G = (V, E)$ with $|V|$ number of vertices, let $A = (a_{v,t})$ be the weighted adjacency matrix. The relative centrality score of vertex v can be defined as:

$$x_v = \frac{1}{\lambda}\sum_{t \in V} a_{v,t} x_t \quad , \tag{2}$$

which can be rearranged in a matrix form as

$$\lambda x = Ax. \tag{3}$$

Given the requirement that all entries in x must be non-negative, the Perron-Frobenius theorem implies that only the greatest eigenvalue results in a proper centrality measure (Newman 2010). Hence, the centrality measure is given by the eigenvector associated with the largest eigenvalue of the connectivity matrix. Then, the ith contact is assigned the ith component of this eigenvector where i goes from 1 to number of recording sites in a patient. The eigenvector centrality is by definition a self-referential measure of centrality, i.e., nodes have high eigenvector centrality if they connect to other nodes that have high eigenvector centrality (Rubinov and Sporns, 2010), which ultimately provides a measure of relative importance of each node in the network. The eigenvector centrality measure has been applied

to resting-state fMRI studies (Lohmann *et al.*, 2010) and more recently to ECoG recordings of epileptic patients (Burns *et al.*, 2014).

By computing the centrality in each 0.6s-long connectivity matrix we obtained for each patient independent eigenvector centrality sequences along each recording session. If we consider each connectivity matrix to represent a brain state (Allen *et al.*, 2014), these vectors can be regarded as representative elements of these states in a vector space of dimension equal to the number of recording sites. Further, these vectors point to the direction that best summarizes the original brain state. In particular, every time that a significant change arises in the connectivity matrix, the eigenvector centrality rotates to update the relative importance ("centrality") of each contact within the new network configuration.

Our goal was to evaluate the variability of these representative states in each period. The long sequence of centrality vectors for each period can be equivalently regarded as a stream of simultaneous centrality time series, one for each recorded contact. Then, one can evaluate the spatio-temporal variability of the centrality time series through the application of the multivariate Gaussian entropy (Cover and Thomas, 2012) in a given estimation time window that we choose for this study to be 120s. The multivariate Gaussian entropy is defined as

$$H_c = \frac{k}{2}\left(1 + \ln(2\pi)\right) + \frac{1}{2}\ln\det(\Sigma), \tag{4}$$

where k is the number of recording sites, and $\sum$ is the covariance matrix of the centrality time series estimated in a the estimation windows. By considering centrality vectors to be independent, $\sum$ in (4) becomes a diagonal matrix, and the Gaussian entropy captures the aggregated variability of the centrality vectors across the temporal dimension:

$$H_c^{(1)} = \frac{k}{2}\left(1 + \ln(2\pi)\right) + \frac{1}{2}\sum_{i=1:k}\ln\Sigma_{i,i}. \tag{5}$$

By subtracting (5) from (4), one can evaluate the variability of the centrality vectors across the spatial dimension:

$$H_c^{(2)} = \frac{1}{2}\left(\ln\det\Sigma - \sum_{i=1:k}\ln\Sigma_{i,i}\right). \tag{6}$$

Hence, the two contributions sum up to give the Gaussian entropy (4):

$$H_c = H_c^{(1)} + H_c^{(2)} \tag{7}$$

State clusterization

To associate the network variability decreased observed in all patients with the occurrence of certain connectivity states, we jointly clustered the eigenvector centrality sequences in the pre-seizure and control periods using the k-means algorithm (Forgy, 1965). We applied this clusterization in patients 1-9 where the number of eigenvector centrality samples was comparable. We fixed the number of clusters to 8 to cover a sufficiently wide range of visually inspected connectivity states per patient.

Statistical analysis

The pre-seizure decrease in centrality entropy was statistically tested as follows. We started by windowing consecutive entropy samples (n=15, 30 minutes) in non-overlapping and paired time segments across each period and then we computed the effect size for each segment pair using Cohen's D (Cohen's D, Cohen, 1992). We then clustered adjacent segments with a criterion of effect size being larger of 0.15 (low-medium effect, Cohen, 1992) over a minimum of 4 adjacent segments (2 hours), and considered the aggregated sum of these segments' effect sizes as the main statistic. We further checked the statistical significance of this value through non-parametric statistical testing based on Monte Carlo sampling (Maris and Oostenveld, 2007). More concretely, for each patient with time segments satisfying the above criterion, we computed 1,000 random permutations of the centrality entropy samples across both conditions (within pre-seizure or control period) at each time segment, and repeated the same segment clusterization procedure to obtain 1000 surrogate statistic values. These values were used to approximate a null distribution against which we compared the original aggregated effect size value via a right-tail sided significance test. If the test's significance value was below 0.05, we considered the pre-seizure interval formed by the adjacent segments to exhibit significantly lower centrality entropy than the one obtained in the control period and we identified it as a *critical phase*. In addition, we made use of the Kolmogorov Smirnov test to assess that the critical phase distribution across patients was significantly different from a distribution of randomly placed significant clusters of the same duration.

In general, to test differences across time (pre-seizure vs. control period) or recording sites (Epileptogenic zone vs. non-epileptogenic zone) samples, we made use of the effect size based on Cohen's D for small and non-comparable number of samples, the paired Wilcoxon test for small sample sizes, the paired t-test for sufficiently large number of samples. We resorted to partial correlations to evaluate the marginal contribution of the centrality entropy decrease with the temporal frequency of each clusterized state in patients 1-9. Finally, mean connectivity values across electrode pairs were computed using the Fisher transform (Fisher, 1920).

Acknowledgements

We would like to thank Dr. Ralph Andrzejak, Dr. Maria Victoria Puig and Dr. Thomas Gener for their insightful comments during the preparation of this manuscript.

Funding

G.D. was supported by the European Research Council Advanced Grant DYSTRUCTURE (Grant 295129) and by the Spanish Research Project SAF2010-16085. A.T.C. was supported by the European Community's Seventh Framework Programme (FP7/2007-2013) under Grant Agreement PEOPLE- 2012-IEF-329837.

Author contributions

A.T.C. and A.P. acquired the data; A.T.C. analysed the data and wrote the manuscript. All authors contributed to the design of the study paradigm and the interpretation of the results.

Competing financial interests

The authors declare no competing financial interests.

References

Andrzejak RG, Mormann F, Kreuz T, Rieke C, Kraskov A, Elger CE at al Testing the null hypothesis of the nonexistence of a preseizure state. *Physical Review. E, Statistical, Nonlinear, and Soft Matter Physics.* 2013;67(1 Pt 1), 10.1103/PhysRevE.67.010901

Allen EA, Damaraju E, Plis SM, Erhardt EB, Eichele T, Calhoun VD. Tracking whole-brain connectivity dynamics in the resting state. *Cereb Cortex*. 2014;24(3):663-676. 10.1093/cercor/bhs352

Bartolomei F, Gavaret M, Hewett R, et al. Neural networks underlying parietal lobe seizures: A quantified study from intracerebral recordings. *Epilepsy Res*. 2011;93(2-3):164-176. 10.1016/j.eplepsyres.2010.12.005

Brinkman B, Wagenaar J, Abbot D, Adkins P, Bosshard S, et al. Crowdsourcing reproducible seizure forecasting in human and canine epilepsy. *Brain*. 2016;139(6), 1713-1722. 10.3102/0002831212437854

Burns SP, Santaniello S, Yaffe RB, Jouny CC, Crone NE, Bergey GK, et al. Network dynamics of the brain and influence of the epileptic seizure onset zone. Proc Natl Acad Sci 2014; 111: 5321-30. 10.1073/pnas.1401752111

Centers for Disease Control and Prevention (CDC) "Epilepsy in adults and access to care--United States, 2010." MMWR. Morbidity and mortality weekly report 2012 61.45: 909.

Cohen J. A power primer. *Psychol Bull*. 1992;112(1):155-159.

Cook MJ, O'Brien TJ, Berkovic SF, et al. Prediction of seizure likelihood with a long-term, implanted seizure advisory system in patients with drug-resistant epilepsy: A first-in-man study. *Lancet Neurol*. 2013;12(6):563-571. 10.1016/S1474-4422(13)70075-9

Cossu M, Fuschillo D, Casaceli G, Pelliccia V, Castana, et al. Stereoelectroencephalography-guided radiofrequency thermocoagulation in the epileptogenic zone: a retrospective study on 89 cases. *J Neurosurg*. 2015; 1-10.

Cover TM, Thomas JA. *Elements of information theory*. John Wiley & Sons, 2012.

Damaraju E, Allen EA, Belger A, Ford JM, McEwen S, et al. Dynamic functional connectivity analysis reveals transient states of dysconnectivity in schizophrenia. *NeuroImage: Clinical*. 2014. *5*(July), 298–308. 10.1016/j.nicl.2014.07.003

David O, Blauwblomme T, Job AS, Chabardès S, Hoffmann D, Minotti L, et al. Imaging the seizure onset zone with stereo-electroencephalography. *Brain.* 2011; 134(Pt 10): 2898-911.

Deco G, Kringelbach ML. Great expectations: Using whole-brain computational connectomics for understanding neuropsychiatric disorders. *Neuron*. 2014. 84(5), 892–905. http://doi.org/10.1016/j.neuron.2014.08.034

Dimitriadis SI, Laskaris NA, Del Rio-Portilla Y, Koudounis GC. Characterizing dynamic functional connectivity across sleep stages from EEG. *Brain Topography*. 2009;*22*(2), 119–133. 10.1007/s10548-008-0071-4

Draguhn A, Traub RD, Schmitz D, Jefferys JGR. Electrical coupling underlies high-frequency oscillations in the hippocampus in vitro. *Nature.* 1998; 394: 189-192.

Fischl B. FreeSurfer. *Neuroimage* 2012; 62:774-81.

Fisher RA. Frequency distribution of the values of the correlation coefficient in samples from an indefinitely large population. *Biometrika*.1914, 10(4), 507-521.

Forgy EW. Cluster analysis of multivariate data: efficiency versus interpretability of classifications. *Biometrics.* 1965; 21: 768-69.

Gadhoumi K, Lina JM, Mormann F, Gotman J. Seizure prediction for therapeutic devices: A review. *J Neurosci Methods*. 2015;(029):1-13. 10.1016/j.jneumeth.2015.06.010

Geier C, Lehnertz K, Bialonski S. (2015). Time-dependent degree-degree correlations in epileptic brain networks: from assortative to dissortative mixing. *Frontiers in Human Neuroscience*, *9*(August), 462. 10.3389/fnhum.2015.00462

Goodfellow M, Rummel C, Abela E, Richardson MP, Schindler K, et al. (2016). Estimation of brain network ictogenicity predicts outcome from epilepsy surgery. *Scientific Reports*. 2016;6:1-13.

Hudetz AG, Liu X, Pillay S. Dynamic Repertoire of Intrinsic Brain States Is Reduced in Propofol-Induced Unconsciousness. *Brain Connect*. 2015;5(1):10-22.

Hutchison RM, Womelsdorf T, Allen EA, et al. Dynamic functional connectivity: Promise, issues, and interpretations. *Neuroimage*. 2013;80:360-378.

Jiruska P, de Curtis M, Jefferys JGR, Schevon CA, Schiff SJ, Schindler K. Synchronization and desynchronization in epilepsy: controversies and hypotheses. *J Physiol*. 2013;591(4):787-797. 10.1113/jphysiol.2012.239590

Khambhati, A. N., Davis, K. A., Oommen, B. S., Chen, S. H., Lucas, T. H., Litt, B., & Bassett, D. Dynamic network drivers of seizure generation, propagation and termination in human neocortical epilepsy. *PLoS Comput Biol*. 2015;11(12) 1-19. 10.1371/journal.pcbi.1004608

Khambhati AN, Davis KA, Lucas TH, Litt B, Bassett DS. Virtual cortical resection reveals push-pull network control preceding seizure evolution. *Neuron*. 2016:91(5), 1170-1182.

Kramer, M. A., Kolaczyk, E. D., & Kirsch, H. E. Emergent network topology at seizure onset in humans. *Epilepsy Research*. 2008;*79*(2-3), 173–186. 10.1016/j.eplepsyres.2008.02.002

Kramer MA, Eden UT, Lepage KQ, Kolaczyk ED, Bianchi MT at al. Emergence of persistent networks in long-term intracranial EEG recordings. *J Neurosci 2011*; 31:15757-67.

Kerr MS, Burns SP, Gale J, Gonzalez-Martinez J, Bulacio J, Sarma SV. Multivariate analysis of SEEG signals during seizure. In *2011 Ann Int Conf IEEE Eng Med Biol Soc.* 2011; 8279-82.

Kuhnert, M.-T., Elger, C. E., & Lehnertz, K. (2010). Long-term variability of global statistical properties of epileptic brain networks. *Chaos 20*(2010),043126. 10.1063/1.3504998

Jones DT, Vemuri P, Murphy MC, Gunter JL, Senjem ML, et al. Non-stationarity in the "resting brain's" modular architecture. *PLoS ONE*. 2012;*7*(6).

Le Van Quyen M, Soss J, Navarro V, et al. Preictal state identification by synchronization changes in long-term intracranial EEG recordings. *Clin Neurophysiol*. 2005;116(3):559-568. 10.1016/j.clinph.2004.10.014

Liao W, Zhang Z, Mantini D, et al. Dynamical intrinsic functional architecture of the brain during absence seizures. *Brain Struct Funct*. 2014;219(6):2001-2015. 10.1007/s00429-013-0619-2

Lohmann G, Margulies DS, Horstmann A, et al. Eigenvector centrality mapping for analyzing connectivity patterns in fMRI data of the human brain. *PLoS One*. 2010;5(4). 10.1371/journal.pone.0010232

Lopes da Silva F, Blanes W, Kalitzin SN, Parra J, Suffczynski P, Velis DN. Epilepsies as dynamical diseases of brain systems: basic models of the transition between normal and epileptic activity. *Epilepsia.* 2003;44 (Suppl 12): 72–83.

Maris E, Oostenveld R. Nonparametric statistical testing of EEG- and MEG-data. *J Neurosci Methods*. 2007;164(1):177-190. 10.1016/j.jneumeth.2007.03.024

Mirowski P, Madhavan D, LeCun Y, Kuzniecky R. Classification of patterns of EEG synchronization for seizure prediction. *Clin Neurophysiol.* 2009; 120: 1927-40.

Morgan VL, Abou-Khalil B, Rogers BP (2014). Evolution of Functional Connectivity of Brain Networks and Their Dynamic Interaction in Temporal Lobe Epilepsy. *Brain Connectivity.* 2014;*5*(1):35–44.

Mormann F, Kreuz T, Andrzejak RG, David P, Lehnertz K *et al.*, C. E. Epileptic seizures are preceded by a decrease in synchronization. *Epilepsy Research*. 2013;*53*(3), 173–185. 10.1016/S0920-1211(03)00002-0

Mormann F, Andrzejak RG, Elger CE, Lehnertz K. Seizure prediction: the long and winding road. *Brain.* 2007; 130 (Pt 2): 314-33. 10.1093/brain/awl241

Newman MEJ. Networks: An introduction. Oxford University Press; 2010. 10.1057/9780230226203.1064

Park Y, Luo L, Parhi KK, Netoff T. Seizure prediction with spectral power of EEG using cost-sensitive support vector machines. *Epilepsia*. 2011;52(10):1761-1770. 10.1111/j.1528-1167.2011.03138.x

Patrick K, Schachter SC, Brodie MJ. Drug-resistant epilepsy. N Engl J Med 2011; 365: 919-26.

Pereda E, Quiroga RQ, Bhattacharya J. Nonlinear multivariate analysis of neurophysiological signals. *Prog Neurobiol* 2005; 77:1-37.

Ponten SC, Bartolomei F, Stam, CJ. Small-world networks and epilepsy: graph theoretical analysis of intracerebrally recorded mesial temporal lobe seizures. *Clin Neurophysiol.* 2007;118:918-27. 10.1016/j.clinph.2006.12.002

Richardson MP. Large scale brain models of epilepsy: dynamics meets connectomics. *J Neurol Neurosurg Psychiatry*. 2012;83(12):1238-1248. 10.1136/jnnp-2011-301944

Rocamora R, Andrzejak RG, Jimenez-Conde J, Elger CE. Sleep modulation of epileptic activity in mesial and neocortical temporal lobe epilepsy: A study with depth and subdural electrodes. Epilepsy and Behavior 2013; 28 (2):185-190.

Rubinov M, Sporns O. Complex network measures of brain connectivity: uses and interpretations. Neuroimage 2010; 52: 1059-69.

Rummel C, Goodfellow M, Gast H, Hauf M, Amor F, et al. A systems-level approach to human epileptic seizures. *Neuroinformatics*. 2013;11(2), 159-173. 10.1007/s12021-012-9161-2

Santaniello S, Sherman DL, Thakor NV, Eskandar EN, Sarma SV. Optimal control based Bayesian detection of clinical and behavioral state transitions. IEEE Trans Neural Syst Rehabil Eng 2012; 20: 708–19.

Stacey W, Le Van Quyen M, Mormann F, Schulze-Bonhage A. What is the present-day EEG evidence for preictal state? *Epilepsy Res*. 2011;97(3):243-251. 10.1016/j.eplepsyres.2011.07.012

Stam CJ. Modern network science of neurological disorders. *Nat Rev Neurosci.* 2014;15:683-95. 10.1038/nrn3801

Stefan H, da Silva FHL. Epileptic neuronal networks: methods of identification and clinical relevance. *Front Neurol.* 2013; 4.

Takahashi H, Takahashi S, Kanzaki R, Kawai K. State-dependent precursors of seizures in correlation-based functional networks of electrocorticograms of patients with temporal lobe epilepsy. *Neurol Sci.* 2012;33:1355-64. 10.1007/s10072-012-0949-5

Tagliazucchi E, Carhart-Harris R, Leech R, Nutt D, Chialvo DR. Enhanced repertoire of brain dynamical states during the psychedelic experience. *Hum Brain Mapp*. 2014;35(11):5442-5456. 10.1002/hbm.22562

Valderrama MC, Alvarado C, Nikolopoulos S, Martinerie J, Adam C, Navarro V, et al. Identifying an increased risk of epileptic seizures using a multi-feature EEG–ECG classification. *Biomed Sig Proc and Control.* 2012;7:237-44.

Van Diessen E, Diederen SJH, Braun KPJ, Jansen FE, Stam CJ. Functional and structural brain networks in epilepsy: What have we learned? *Epilepsia*. 2013;54(11):1855-1865. 10.1111/epi.12350

Van Mierlo P, Carrette E, Hallez H, et al. Ictal-onset localization through connectivity analysis of intracranial EEG signals in patients with refractory epilepsy. *Epilepsia*. 2013;54(8):1409-1418.

Van Mierlo P, Papadopoulou M, Carrette E, et al. Functional brain connectivity from EEG in epilepsy: Seizure prediction and epileptogenic focus localization. *Prog Neurobiol*. 2014;121:19-35. 10.1016/j.pneurobio.2014.06.004

Wendling F, Ansari-Asl K, Bartolomei F, Senhadji L. From EEG signals to brain connectivity: a model-based evaluation of interdependence measures. *J Neurosci Met.* 2009;183:9-18.

Wilke C, Worrell G, He B. Graph analysis of epileptogenic networks in human partial epilepsy. *Epilepsia.* 2011;*52*(1), 84–93. 10.1111/j.1528-1167.2010.02785.x

Zhang Z, Liao W, Chen H, Mantini D, Ding JR, Xu Q, et al. Altered functional-structural coupling of large-scale brain networks in idiopathic generalized epilepsy. *Brain* 2011;134:2912–28.

Patient	Age/Sex	Recording time (hours)	Epilepsy	Side	MRI	Electrodes (left)	Analyzed regions	Seizures	Epilepsy durations (years)	Surgery	Seizure outcome (Engel's class)	Follow up period
1	31/F	24	TLE	R	negative	5 (0)	A, Ha, Hp, TP, Lateral OFC	FS w CA	10	ATL	1A	3 years
2	26/M	24	TLE	R	right amygdala enlargement	7 (0)	A, Ha, Hp, TP, EC, Lateral OFC, TGi	FS w CA/or FS wo CA	11	RFTC	1A	1.5 year
3	31/F	24	TLE	L	negative	7 (7)	A, Ha, Hp, TP, EC, Lateral OFC, PHCp	FS w CA/or FS wo CA/or FS w CA and tonico-clonic bilateral evolution	25	SAH	1B	3 years
4	39/M	24	PCE	L	reduced size of right hippocampus	10 (8)	A, Ha(2), Hp, TP, EC, POC(2), W, AG	FS w CA/or FS wo CA/or FS w CA and tonico-clonic bilateral evolution	38	temporoparietoocciptal resection	1A	5 months
5	25/M	24.5	PCE	R	right hemispheric atrophy	15 (0)	TP, A, Ha, Hp, EC, POC(2), W, AG, Ia, Im, Ip, Lateral OFC, M1	FS w CA/or FS w CA and tonico-clonic bilateral evolution	16	temporoparietoocciptal resection	1B	2 months
6	45/M	24	TLE	L	negative	12 (12)	A, Ha, Hp, TP, EC, iTG, Ia, Ip, TPCp, HS, FB, CGp	FS w CA/or FS w CA and tonico-clonic bilateral evolution	36	RFTC	1A	3 months
7	30/M	23,2	TLE	L	reduced size of left hippocampus	9 (8)	A, Ha(2), Hp, TP, EC, W, PHCp, TOJ	FS w CA/or FS w CA and tonico-clonic bilateral evolution	10	NO	_	_
8	23/M	24	TLE	R	right temporal polar blurring	15 (0)	A, Ha, Hp, TP, EC, PHCp, W, B, TOJ (2), TGs, Lateral OFC (4)	FS w CA/or FS w CA and tonico-clonic bilateral evolution	7	RFTC	1A	3 months
9	40/M	24	TLE	L	left temporal polar blurring	8 (8)	A, Ha, Hp, TP, EC, Lateral OFC, PHCp, TOJ	FS w CA/or FS wo CA/or FS w CA and tonico-clonic bilateral evolution	38	RFTC	3	1.5 year
10	33/F	8,16	TLE	L	left posterior hippocampal lesion	10(9)	A, Ha(2), Hp, TP, EC, Lateral OFC, PHCp, TOJ, Im	FS w CA/or FS w CA and tonico-clonic bilateral evolution	17	ATL	3	2 years

Table 1. Main data of patients included in the study. F = female; M = male; TLE=temporal lobe epilepsy; PCE=posterior cortex epilepsy; R=right; L=left; A=amygdala; Ha=anterior hippocampus; Hp=posterior hippocampus; TP=temporal pole; EC=entorhinal cortex, Lateral OFC=lateral parts of the orbitofrontal cortex; TGi=inferior temporal gyrus; PHCp=posterior parahippocampal cortex; W=Wernicke's area; AG=angular gyrus; Ia=anterior insula; Im=mid insula; Ip=posterior insula; M1=primary motor area; TPCp=posterior temporoparietal cortex; HS=Heschl's area; FB=frontobasal area; CGp=posterior cingulate; TGs=superior temporal gyrus; TOJ=temporal occipital junction; POC=precuneus occipital cortex; B=Broca's area; FS=focal seizure; w=with; wo=without; CA=consciousness alteration; ATL: Anterior temporal lobectomy; RFTC=Radiofrequency thermocoagulation; SAH=Selective amygdalohyppocampectomy; NO=not-operated;

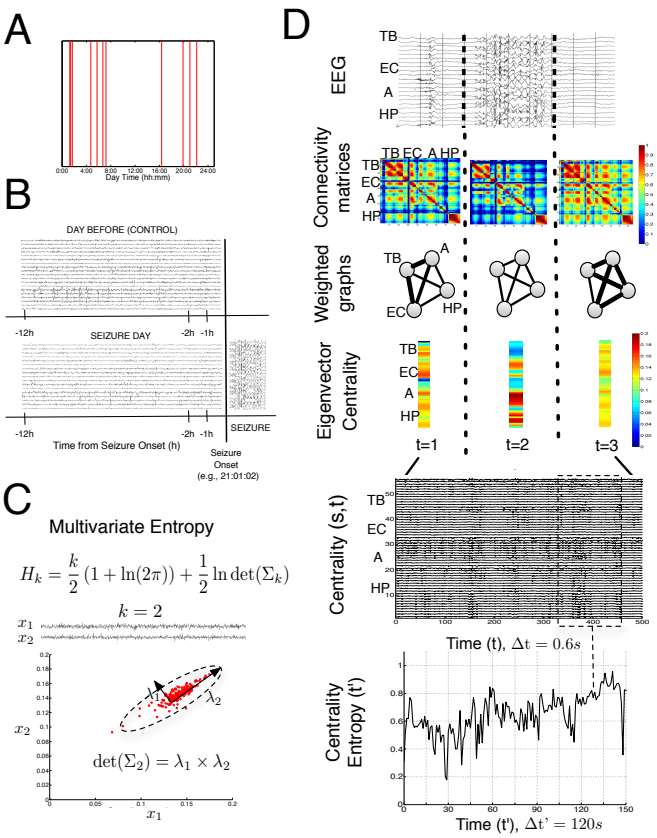

Figure 1. Study paradigm and network dynamics analysis. A: Seizure onset time of the first recorded spontaneous clinical seizure from every patient (n=10). B: Schematic representation of the experimental design: for each patient a pre-seizure period of up to 12 hours was matched to the same time period of the previous day that served as a baseline reference (control interictal period). C: Formula of the multivariate (Gaussian) entropy, showing its dependence on the determinant of the covariance matrix (Σ). Illustration for a bivariate case of how the covariance matrix determines the variability shape of two time series. D: Network dynamics analysis: Simultaneous EEG recordings were first divided into consecutive and non-overlapping time windows of 0.6s (Top). Then, functional connectivity matrices were computed using zero-lagged absolute-valued Pearson correlation in each time windows (Middle-top 1). These matrices were modeled as weighted undirected graphs where nodes represented recorded contacts and edges strength represented correlation absolute values (Middle-top 2). The centrality of each contact in every graph was evaluated using the eigenvector centrality leading to a sequence of centrality vectors (Middle-bottom 1). The overall eigenvector centrality sequence was regarded as a set of simultaneous centrality time series (one for each patient recording site s) over time steps Δt of 0.6s (Middle-bottom 2). Finally, time-dependent centrality entropy values were found for each period of interest by sequentially estimating the multivariate entropy of the centrality time series in non-overlapping and consecutive time windows of 120s (200 samples). The labels TB (Temporal basal area), EC (Entorhinal cortex), A (Amygdala) and HP (Hippocampus) are used as an example to illustrate where the anatomical information was conveyed in each step of the analysis.

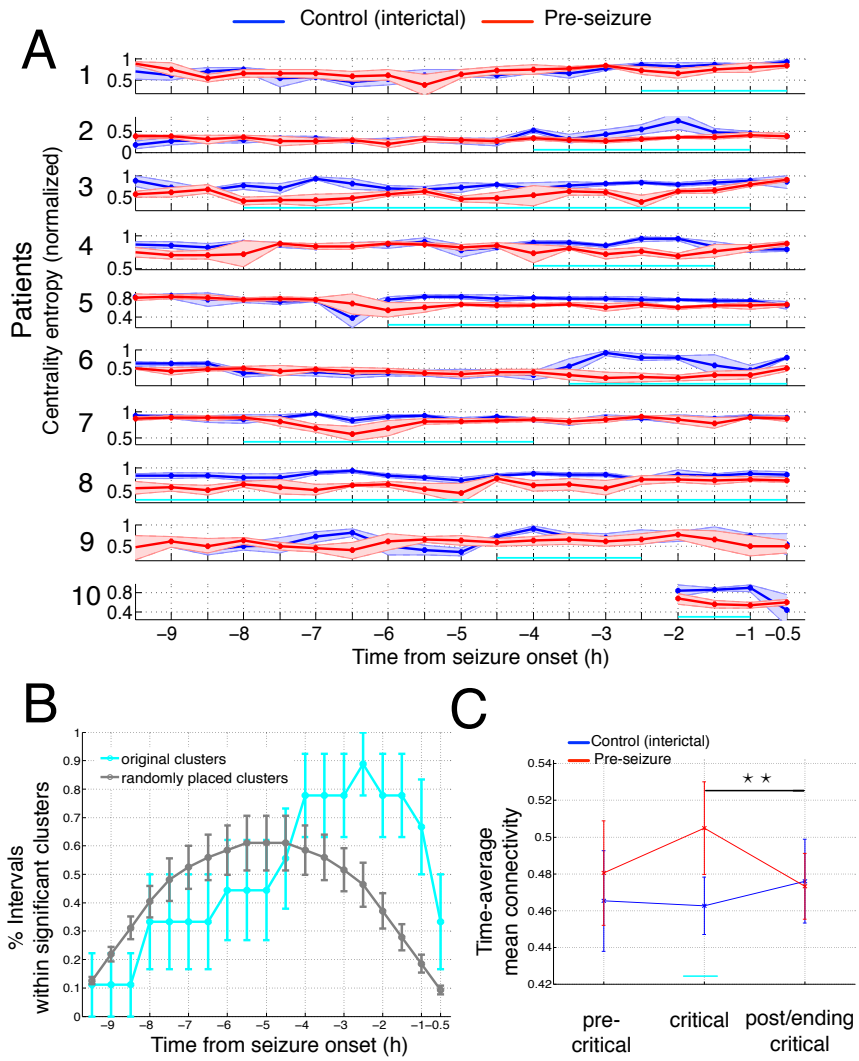

Figure 2. Time-dependent network state variability decreases near seizure onset during pre-seizure periods. A: Average normalized (to the [0,1] range) centrality entropy for 10 epileptic patients during a pre-seizure period (in red, 9.5 hours before the first seizure) and a control period (in blue, 9.5 hours from the preceding day). Averages were computed over time in non-overlapping windows of 15 entropy samples each (total of 30 min) during both periods. Each entropy sample was computed in a smaller window of 200 subsamples (120s). Curves represent the sequence of centrality entropy mean values and error bars denote ± one standard deviation. In cyan, the sequence of consecutive time steps lying in a significant clusterized difference (randomization test, P<0.01). B: Using the first 9 patients, percentage of times that 30-minute intervals lie within a significant cluster. In cyan, significant clusters are located in their original position. In grey, significant clusters are randomly placed along the pre-seizure periods of each patient. Error bars denote SEM (standard error of the mean). C: Median (across patients) of the time-average mean functional connectivity along three consecutive sub-periods of interest during pre-seizure and control periods. The first sub-period (pre-critical) comprises intervals prior to the significant cluster, the intermediate sub-period (critical) comprises intervals within the cluster and the last sub-period (post/ending critical) comprises post-cluster intervals. In patients 1, 6 and 8, in which the critical phase was attached to the seizure onset, the last interval was considered to belong to the post/ending critical. Error bars denote SEM (standard error of the mean). Stars denote that there was a significant difference between the critical and the post/ending-critical sub-periods of the pre-seizure period (P<0.01, Wilcoxon test).**

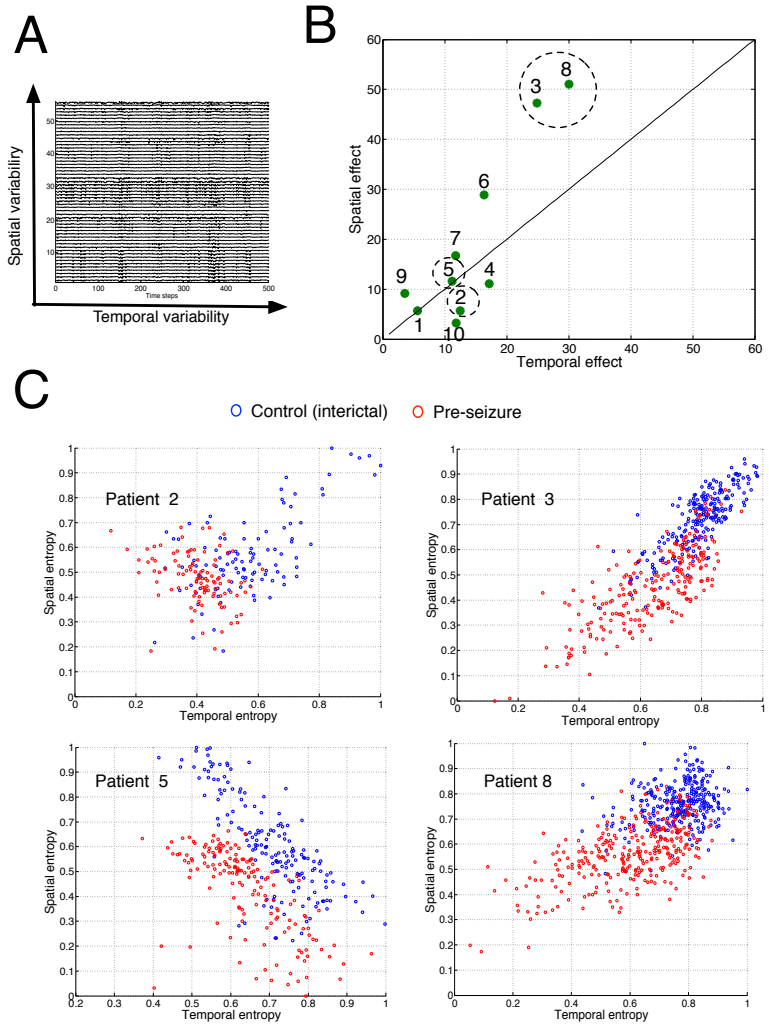

Figure 3. Network state variability reduction across spatial and temporal dimensions. A: Schematic representation of the two sources of variability in a set of simultaneous time series. B: For every patient, green dots representing pairs of statistic values ('temporal/spatial effects') obtained from repeating the clusterized effect-size test (Fig. 3A) with the spatial and temporal entropy respectively. The circled effect pairs are exemplified in Fig. 3C. C: For exemplary patients 2, 3 5 and 8, the figure shows the decomposition of the centrality entropy values into pairs of temporal and spatial entropy values. In blue, pairs of entropy values obtained from the control segment. In red, pairs of entropy values obtained from the pre-seizure period.

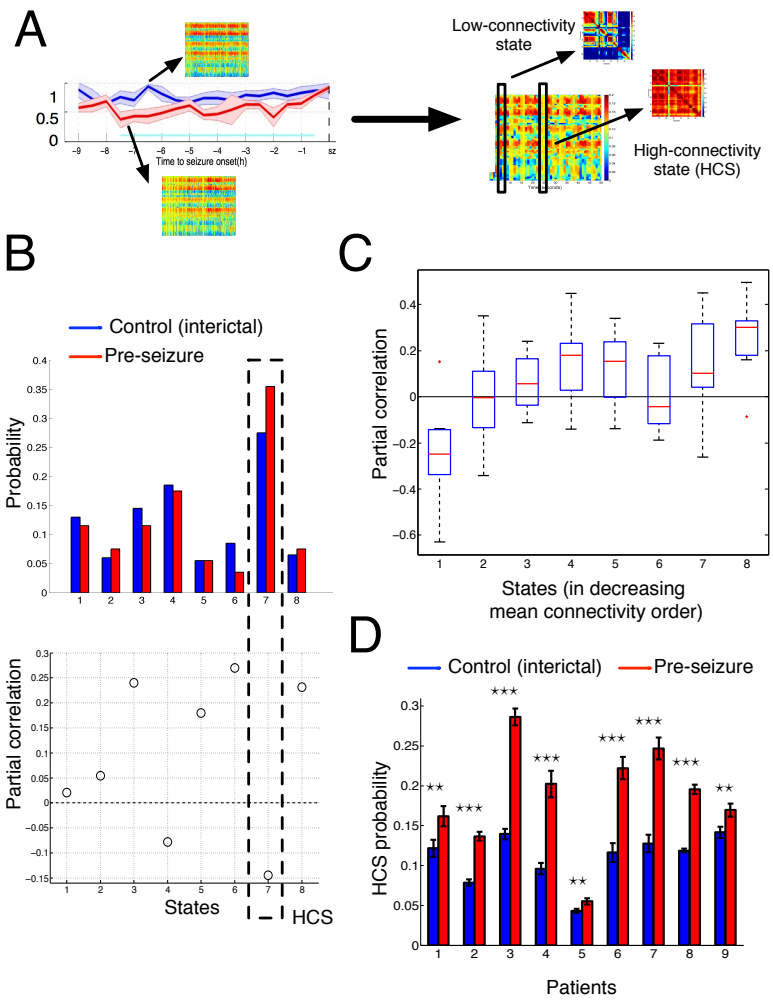

Figure 4: Decrease of network state variability was associated with an increased occurrence of high-connectivity instances (Patients 1-9). A: Visual inspection around the critical phase (in cyan) suggested a higher presence of homogeneous (yellow strips) centrality values during the pre-seizure period (left), which in turn were associated to high-connectivity matrices (High-connectivity states, HCS, right). Color intensity (blue=lowest, red=highest) denotes the centrality of recording sites and connectivity of recording pairs. B: Using data from patient 1, example of discrete states probabilities estimated in the control period (blue) and pre-seizure period (red) over a given time window (Top). For the same patient, each discrete state's probability difference across whole periods was partially correlated with the centrality entropy decrease (Down). The dashed rectangle highlights the probabilities and correlation coefficient of state 7, the state associated with the highest-connectivity matrix in the example presented. The probability state difference and the centrality entropy differences were computed in time windows of 200 time samples (120s) along whole control and pre-seizure periods. C: Contribution of discrete states to the centrality entropy decrease in Patients 1-9. For these patients, discrete states were sorted along the horizontal axis in decreasing order according to the mean connectivity of its associated connectivity matrix. For each sorted state, boxplots show the distribution of the partial correlation values across patients between the probability state difference and the centrality entropy difference. D: High-connectivity state (HCS) probability difference in the critical phase. For each patient, HCS denotes the state associated with the highest connectivity matrix among those states whose probability increase significantly correlated with the entropy decrease. Bars denote the average probability of this state during the critical phase of the pre-seizure (red) and control periods (blue) per patient. Error bars denote ± one standard error of the mean (SEM). Upper stars show that the differences in HCS probabilities were significant in all studied patients (P<0.01, *** P<001, paired t-test).**

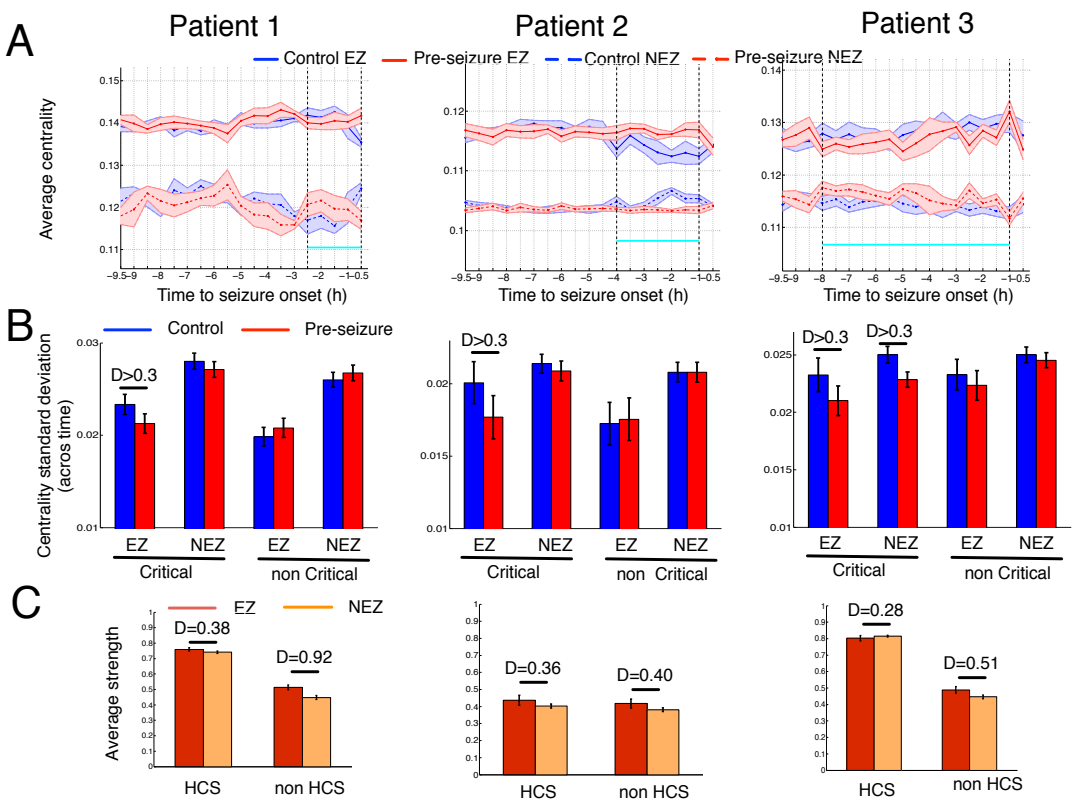

Figure 5: Decrease of network state variability was related to the epileptogenic zone of patients with very good post-surgical outcome (Engel 1A and 1B, minimal follow-up of 1.5 years, Table 1). In every patient the epileptogenic zone (EZ) was considered to include the resected zone (after resectomy in patients 1 and 3, and after RFTC in patient 2) and the clinically diagnosed seizure onset zone. A: For each patient and period, site-average eigenvector centrality in the EZ and in the non-epileptogenic zone (NEZ), averaged within non-overlapping and consecutive time windows of 120s (200 samples) during 9.5 hours prior to seizure onset time. In solid line, average centrality of the EZ. In dashed line, average centrality of the NEZ. Blue and red curves stand for the control and pre-seizure periods respectively. For illustration purposes, curves were averaged within windows of 30 minutes (15 samples per window) to enable direct comparison with the estimated critical phase (highlighted in cyan between two dashed vertical lines). Error bars denote ±one standard deviation. B: For each patient, bars showing the site-average standard deviation of the eigenvector centrality in the EZ and NEZ compared across recording periods (control in blue, pre-seizure in red) inside (critical, left) and outside (non critical, right) the estimated critical phase (cyan segment in A). Each sample per recording site was computed by preforming an average (across pre-ictal and non critical phases) of the centrality's standard deviation measured in non-overlapping and consecutive time windows of 120s (200 samples). To correct for the different sample sizes associated with EZ and NEZ, significant differences between periods were reported if the effect size measured with "Cohen's d" (D) was larger than 0.3 (Cohen, 1992). Error bars denote ±SEM. C: Effect of high-connectivity state into the epileptogenic zone. For each patient, bars showing the site-average connectivity strength of the EZ and NEZ during the high-connectivity clusterized states (HCS, left) of each patient and during the remaining states (non HCS, right). Strength samples were computed for each site by performing averages over each segment (HCS and non HCS) during the pre-seizure period. Effect sizes were reported using "Cohen's d". Error bars denote ±SEM.